



Nanosized Calcium-Deficient Carbonated Hydroxyapatite synthesized by microwave activation

Z. Gandou^{1,2*}, A. Nounah¹, B. Belhorma², A. Yahyaoui³

1 : Laboratory of Energy, Materials and Environment, High School of technology , B.P. 227, Salé, Avenue Prince Héritier, Maroc,

2: Laboratory of Chemistry, cell Materials Sciences, CNESTEN, BP 1382 Rabat Principal Morocco.

3 : Laboratory of Radiochemistry and Nuclear Chemistry, Faculty of Sciences B.P. 1014 RP, Rabat, Morocco.

Received 19 July 2014, Revised 22 Oct 2014, Accepted 23 Oct 2014

*Corresponding Author. E-mail: Zahra.gandou@gmail.com; Tel: (+212651628626)

Abstract

Calcium phosphates are essential components in the development of bioactive materials because of their perfect biocompatibility, their ability to bio-degradation and their biological reactivity. In fact, their chemical compositions are similar to the hard tissue of bone and teeth. We are interested in the synthesis of a calcium phosphate-carbonated apatite. Its biological properties, its availability and low cost as well as its physico-chemical properties. In our work a template free and in atmospheric conditions using microwave-precipitation method was successfully developed for the synthesis of nanosized carbonated hydroxyapatite (CHA), which enables to synthesize the ultra fine and high purity powders in short time. The prepared CHA were characterized by means of X ray diffraction (XRD), Fourier transform infrared spectroscopy (FTIR), transmission electron microscopy (TEM) as dried and after calcination. TEM images showed a clear spherical morphology nanoparticles with diameter around 66 nm before calcination which increase of size after calcination is around 180 nm. The XRD and FTIR indicated a typical carbonated hydroxyapatite phase with high cristallinity after calcination.

Keywords: Co-precipitation, microwave activation, carbonated hydroxyapatite, nanospheres, calcination.

1. Introduction

Hydroxyapatite (HA) and β tricalcium phosphate (β TCP) are currently the main components used to synthesize the orthopedic bioceramics. Their chemical compositions very similar to the mineral phase of bone, their biological properties and their biocompatibility make them excellent substitutes bone [1]. But it is difficult to make the high purity HA because of calcium phosphates have many derivates and the synthesis of calcium phosphates strongly dependent on the reaction conditions. However, the mineral composition in human bone differs slightly from stoichiometric HA due to the impurities in human bone, which include the following ions: carbonate, chloride, fluoride, magnesium, and sodium [2-5]. Recently, several in vitro studies about carbonated hydroxyapatite (CHA) are investigated. R. Murugan and al have demonstrated that the in vitro solubility of carbonated hydroxyapatite under physiological conditions is appreciable and is found to be higher than hydroxyapatite (HA), which is a good sign of its bioresorbable nature [6]. Recent study indicated that the dissolution rate of sintered CHA ceramics implanted subcutaneously was intermediate between β tricalcium phosphate (β -TCP) and pure HA [7]. Based on the experimental results, CHA may be a better material for bone substitution than pure HA.

Poorly crystalline apatites (PCA) are the major mineral component of mineralized tissues in vertebrates. Several studies using spectroscopic techniques (Fourier transform infrared [FTIR]; ³¹P nuclear magnetic resonance [NMR]) have demonstrated the existence, both in precipitated and biological PCA, of labile non-apatitic environments of the mineral ions. Their physical-chemical properties are, however, not very well known due to their relative instability and the difficulties to characterize nanocrystalline compounds [8].

Various techniques associating drugs with a calcium phosphate biomaterial have been reported: adsorption and impregnation allow the therapeutic agent to be incorporated at the surface of the biomaterial, whereas centrifugation and vacuum based techniques enable it to enter into pores of biomaterials [9, 10].

El Rhilassi and coauthors concluded that the adsorption and release properties of poorly crystallized calcium phosphates appear strongly dependent on the composition of hydrated surface layer and surrounding

environment and still a great challenge. The understanding of interaction mechanisms and the control of driving forces may provide fundamental tools for development and application of delivery systems based on the adsorption of pharmaceuticals onto calcium phosphates [11]. The study of the phenomenon of adsorption by bioactive calcium phosphate molecules, poorly crystallized showed that this synthetic phosphate apatite structure can act as a carrier drugs in physiological medium [12].

Further investigations indicated that microwave technology has evolved over of last few years this has some advantages such as heating throughout the media, rapid heating, fast reaction, high yield, excellent reproducibility, narrow particle distribution, high purity and high efficient energy transformation, and being environmentally cleaner. Precipitation under microwave irradiation can be influenced by starting pH, ionic concentration, and solution composition [13].

This paper reports the structure study of a products synthesized by template free microwave activation in atmospheric conditions. In this study, the focus is on synthesizing nanosized carbonated apatite able to mimic the morphological and physico-chemical features of biological apatite compounds. Biological apatite is commonly calcium deficient and it is always carbonate substituted. For this reason, it is more appropriate to refer to it as “carbonate apatite” (CA) [14]. The carbonate ions substitute primarily for the phosphate groups of biological apatite, which is designated as Type B substitution. The particles are nanosized with spherical structure prepared by easy low cost way, at short time, needless adjusting pH and in atmospheric ambience.

2. Materials and methods

2.1. Apparatus:

CHA was prepared by co-precipitation of calcium hydroxide ($\text{Ca}(\text{OH})_2$) and phosphoric acid (H_3PO_4), as Ca and P precursors, respectively. In this study, commercially supplied $\text{Ca}(\text{OH})_2$ (99.8% purity) and (H_3PO_4) (85.0–87.0%) and the double distilled water de-ionized water were the only starting materials.

2.2 Synthesis of carbonated apatite and hydroxyapatite:

The aqueous solution of H_3PO_4 0.45M was added to 0.75M aqueous suspension of $\text{Ca}(\text{OH})_2$ in such way that the Ca/P ratio was 1, 67 under a vigorously stirring condition at room temperature for 30 min. The pH was after mixing 11. The reaction can be written as follows: $10\text{Ca}(\text{OH})_2 + 6\text{H}_3\text{PO}_4 \rightarrow \text{Ca}_{10}(\text{PO}_4)_6(\text{OH})_2 + 18\text{H}_2\text{O}$ The mixture was then immediately exposed to microwave radiation (850 W) during 5 minutes.

After microwave exposure, the samples are dried in an oven at 37 °C for 36 hours. These powders were then calcined to 900 °C and holding for 2 h (ramp rate: 5°C/min) to increase their crystallinities and cooled down at room temperature.

Resulting powders were characterized by X-ray diffraction (XRD). The scanning range (2 θ) was from 20° to 70° at a scan speed of 0.1° min⁻¹. Fourier transform infrared spectra (FTIR) were obtained with the wave numbers recorded from 400 to 4000 cm⁻¹ at 2 cm⁻¹ resolution. Small amount of sample powders was blended with KBr and then pressed into discs for the measurement.

The morphology and dimension of the samples were further observed using transmission electron microscopy (TEM).

3. Results and discussion:

3.1. Procedure for lead determination method

The physical and chemical analyses were carried out on the dried precipitate and the powder calcined at 900 °C. The phases formed were identified by the time heating in microwave as dried and after calcination, by infrared spectroscopy (Nicolet AVATAR 360), and X-ray diffraction (SIEMENS D5000, $\lambda_{\text{Cu}}=1.5408 \text{ \AA}$). The software used for data processing of X-ray diffraction was DIFFRACT/AT and the TEM micrographs were obtained on a Tecnai G2 microscope at 120 kV.

4.2 IR characterization

FTIR spectra of carbonated apatite as dried and hydroxyapatite treated at 900°C were shown in Fig.1. For sample as dried the adsorption band of hydroxyl group at 3571 cm⁻¹ disappeared and the bending vibrations of phosphate in 400–600 cm⁻¹ merged into a broad single peak for as dried sample, suggesting its poorly crystalline structure. The broad adsorption at 3441 cm⁻¹ and band at 1636 cm⁻¹ as dried sample is an indication of adsorbed water. The doublet peaks at 1450 and 1420 cm⁻¹ and 873 cm⁻¹ assignable to the doubly degenerated stretching (ν_3) and bending (ν_2) modes of carbonate groups, respectively [15, 17, 18] (Table 1) can be attributed to the vibrational frequencies of carbonate ions substituted at the phosphate site in apatite, so called B-type apatite. The CO_3^{2-} ions absorbed from atmosphere during the synthesis process substituted for the phosphate and as well as the peak weak absorption peaks is assigned to the P-O-H vibration in the HPO_4^{2-} group.

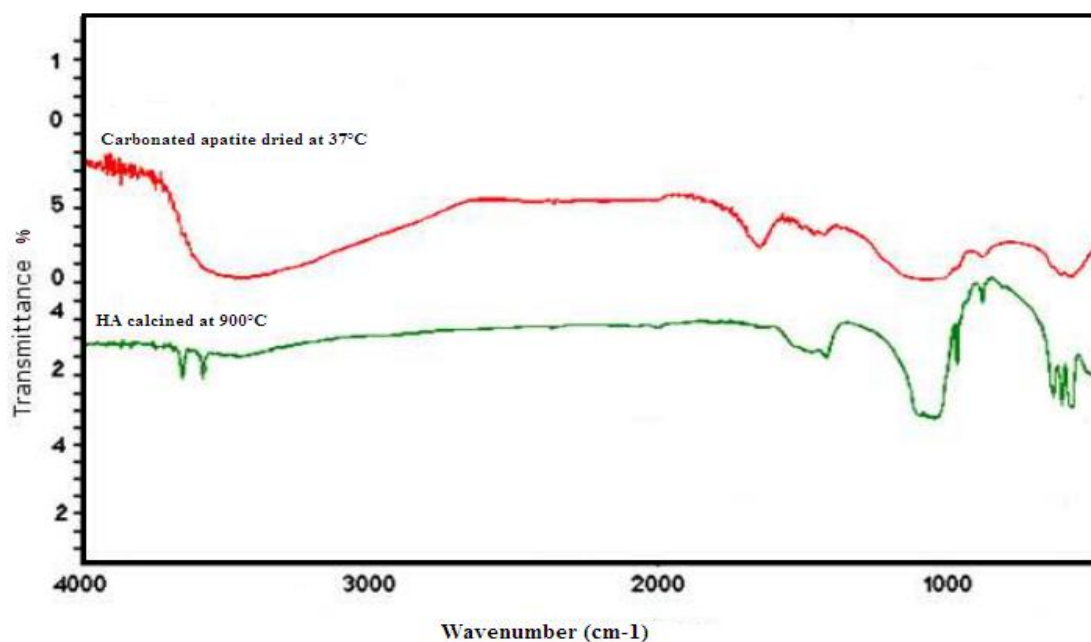


Figure 1: Infrared absorption spectrum of carbonated apatite and HA calcined at 900°C

Table 1: Infrared absorption bands of carbonated apatite as dried and HA after calcination at 900°C.

Absorption bands, cm ⁻¹ As dried	Absorption bands, cm ⁻¹ (900°C)	Attributions	References
-	3571	O-H stretching mode (ν_s) of the OH ⁻ group	[15]
3100- 3441	-	Vibration mode of water	[16]
1636	1650	Deformation of water	[17]
1420- 1448	1413 1450	C-O stretching of carbonate group	[17][18]
1035- 1088	1047 1089	ν_3 asymmetric stretching of P-O bond of PO ₄ ³⁻ group	[15]
961	962	ν_1 P-O symmetric stretching	[18]
873	873	Peak attributed to the vibrational frequencies (ν_2) of carbonate ions substituted at the phosphate site in apatite, so called B-type apatite.	[17] [18]
-	632	ν_L librational mode of hydroxyl group	[15]
563 602	569 602	ν_4 O-P-O Bending modes	[20]
472	434	ν_2 symmetric stretching of P-O bond of phosphate PO ₄ ³⁻ group	[15]

The carbonate content of product should be added here that the molar ratio Ca/(P + C), where C denotes the amount of carbonates, Ca denotes the amount of calcium and P denotes the phosphates amount, should replace the general ratio Ca/P for assessing the global non stoichiometry of carbonated apatite samples [18]. Previous studies showed that calcium phosphates, which are defined by ratio $R = \text{CO}_3^{2-}/(\text{CO}_3^{2-} + \text{PO}_4^{3-})$ between 0 and 0.15 ($1.33 \leq \text{Ca}/\text{P} \leq 1.67$) are poorly crystalline apatite, the crystallization degrades progressively when the ratio $R = \text{CO}_3^{2-}/(\text{CO}_3^{2-} + \text{PO}_4^{3-})$ increases [21]. The sample as synthesized and dried is deficient carbonated poorly crystalline hydroxyapatite which is in good agreement with the XRD result presented in Fig.2. CHA that most closely resemble the mineral phase of biological apatite have been extensively investigated [19].

However for HA treated at 900°C, the obvious phosphate stretching bands at 1089, 1047 and 962 cm⁻¹ and the well-splitting bending bands at 602, 569 and 434 cm⁻¹ proved the structurally ordered (crystal) environment of the PO₄³⁻ groups, which are in agreement with the XRD results. The band at 3571 cm⁻¹ in sample after calcination arises was recorded by Sargin and coauthors [20] and was associated with O-H stretching mode (ν_s) of the hydroxyl group in HA nanomaterials. The intensities of both the hydroxyl bands and the band at 962 cm⁻¹ for phosphate can be used as indication of the HA [22]. The absorption bands observed of powder after sintering

are similar to infrared absorption bands of carbonated apatite 1650 cm^{-1} and 1413 cm^{-1} and 873 cm^{-1} that are attributed to incorporation of CO_3^{2-} ions because the reaction of CO_2 present in the atmosphere.

The FTIR results indicated that the product treated at 900°C sample is nanosized carbonated hydroxyapatite. After sintering, the bands of CHA becomes more and more obvious sharpening which indicated the improvement of the crystalline and the increase of particle size and decrease of amount of carbonates which reflects the effect of calcination.

4.2 XRD characterization

The XRD patterns of as-dried and after calcination samples are shown in Fig. 2 and Fig. 3, respectively. On Fig. 3, we can see that the HA sample demonstrated some weak diffraction peaks that match those of standard HA (JCPDS NO. 9- 0342). Considering the XRD results, we can conclude that the particles of powder as synthesized showed in Fig.2 were poorly crystalline calcium phosphate and after calcination Fig. 3 the crystallinity increases as shown by the sharp peaks in XRD pattern of calcined sample.

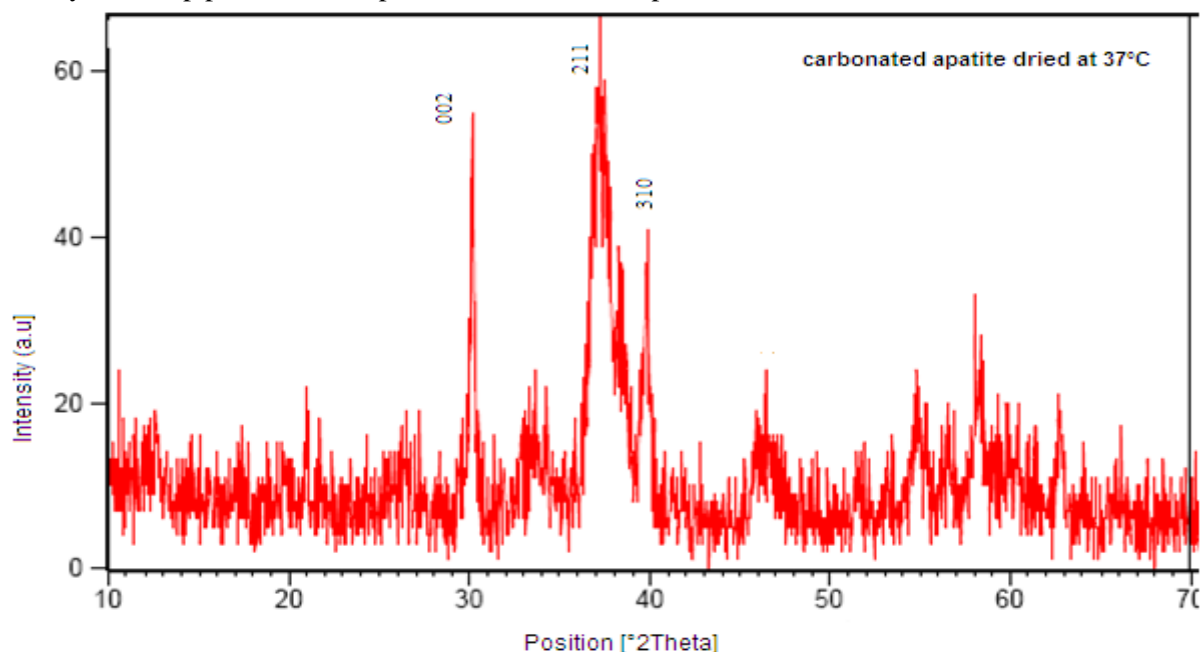


Figure 2: XRD pattern of carbonated apatite synthesized by microwave as dried

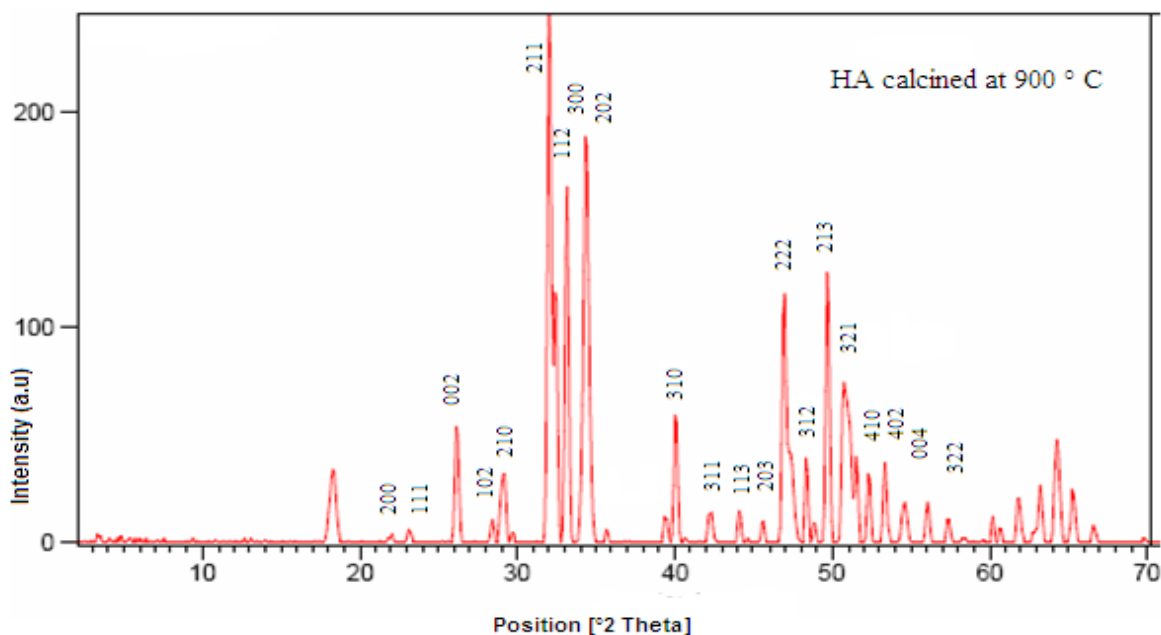


Figure 3: XRD pattern of Hydroxyapatite after calcination at 900°C .

4.3 Transmission electron microscopy “TEM” characterization:

The shape, size, and morphology of calcium phosphates powders as dried and after calcinations at 900°C were revealed by Transmission electron microscopy “TEM” (illustrated respectively in Fig.4 and Fig.5). The micrographs shows that synthesized powders exist as spherulites agglomerates in nanometric scale.

The sample as dried becomes fine with grain size around 66 nm and the particle size is uniform, more homogeneous and highly agglomerated. Such assembly phenomenon also requires extra energy, which is consequently inhibited in microwave irradiation. However, during the period of cooling down, these nanospheres start fusing to each other [13]. This assembly of nanoparticles of calcium phosphate may provide information on the growth kinetics of calcium phosphates. In literature, a model involving aggregation-based growth [23] recently challenged the conventional concept for crystal growth. Inorganic nano-sized crystals were found to aggregate into ordered solid phases via oriented attachment to control the reactivity of nanophase materials in nature [24, 25]. A model of “bricks and mortar” was suggested to explain the biological aggregation of nano-sized apatite[26]. In this model, ACP acts as “mortar” to cement the crystallized “bricks” of nano-sized HA. Meanwhile, biological molecules control the construction process. By using nanodimensional spheres of HA as the building blocks, highly ordered enamel-like and bone-like apatites were hierarchically constructed in the presence of glycine and glutamate, respectively. It is interesting that, during the evolution of biological apatite, the amorphous “mortar” can be eventually turned into the “brick” by phase-to-phase transformation to ensure the integrity of biominerals[26].

Several researchers found evidences that strongly support this aggregation mechanism to explain HA formation. The mechanism proposed by Melikhov [27] can be divided into the following steps:

- a) homogeneous nucleation of ACP;
- b) aggregation of primary ACP particles into typically spherical units;
- c) aggregation of spheres into chain-like structures;
- d) growth of these structures;
- e) Secondary precipitation and phase transformation. The initially precipitated particles of the amorphous phase were observed to be round-shaped with 20–30 nm in size and they can reach 120 nm in size [28].

Nanoparticles after calcination at 900°C reveal that the material with spherical shape has fused together building clearly visible sinter necks and are much larger than primary particles of approximately 180 nm.

Calcination has no significant impacts on the morphology of formed nanospheres.

Spherical morphology is desired for a number of reasons. Firstly, spherical particles have large surface areas for superior binding properties with other materials. Secondly, particles with this property as shown in several study, generate lower backpressure and have greater mechanical stability.

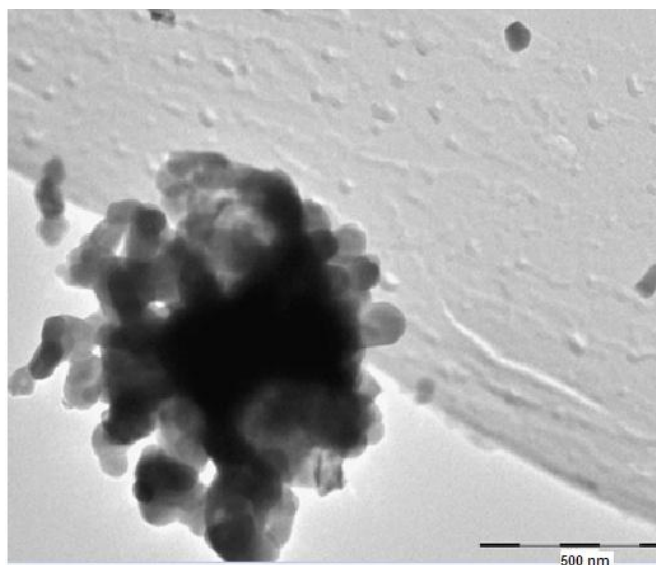


Figure 4: TEM image of carbonated apatite synthesized by microwave as dried

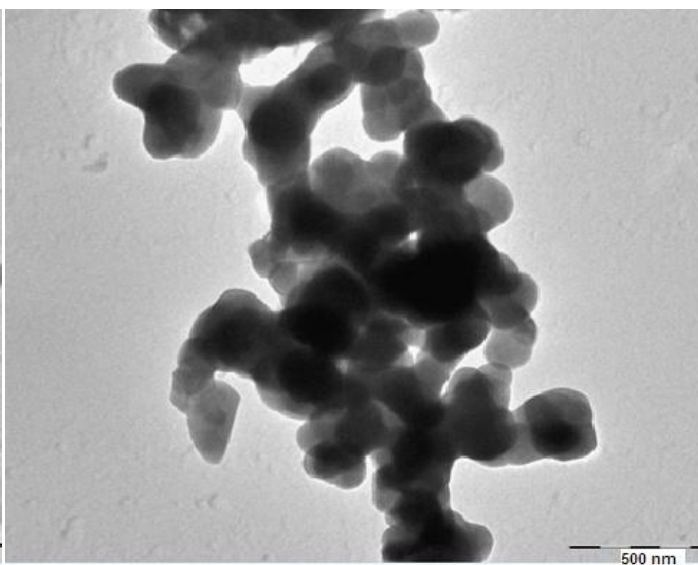


Figure 5: TEM image of Hydroxyapatite after calcination at 900 °C

Conclusion

In this study, we have demonstrated that microwave assisted method as source of activation for synthesis and using lime and phosphoric acid as precursors, is remarkably simple and does not require adjustment of pH or inert atmospheres to produce nanosized carbonated apatite. The microwave can act as quick and homogeneous heater, which provides a unique platform for heating and the growth of novel nanostructures.

Calcination has no significant impacts on the morphology of formed nanospheres.

Since, the substitution of carbonate ion into apatite phase is obvious by the present method during the formation and after calcinations of spherical nanosized particles, it is anticipated to form implant mimicking bone in structure and size.

References

1. Hench L. L. *J. AM. Ceram. Soc.*, 74 13 1 (1991) 1487-1510.
2. Shpak A.P., Karbovskii V.L., Vakh A.G. *J. Electron. Spectrosc.* 585 (2004) 137–140.
3. Sudarsanan K., Young R.A. *Acta Cryst.*, B34 (1978) 1401.
4. Laghzizil A., El Herch N., Bouhaouss A., Lorente G., Macquete J. *J. Solid State Chem.*, 60 (2001) 156.
5. Kannan S., Rebelo A., Ferreira J.M.F. *J. Inorg. Biochem.* 100 (2006) 1692.
6. Murugan R., Ramakrishna S., Rao K. P., *Materials Letters* 60 (2006) 2844–2847.
7. Lange G.L.D., Putter C.D., Groot K.D., *Biomater. Biochem.*, 5 (1983) 451–462.
8. Cazalbou S, Combes C., Eichert D., Rey C., Glimcher M.J. *J. Bone Miner. Metab* 22(2004)310-317.
9. Gautier H., Daculsi G. & Merle C. *Biomaterials* ,22, 18 (2001) 2481-7
10. Gautier H. , Merle , C. ,Auget J.L. & Daculsi G. *Biomaterials* 21 , 3 (2000) 243-249
11. El Rhilassi A., Mourabet M., El Boujaady H., Ramdane H., Bennani-Ziatni,M. , El Hamri R., Taitai A., *J. Mater. Environ. Sci.* 3 (3) (2012) 515–524.
12. El Rhilassi A., Mourabet M., El Boujaady H., Bennani Ziatni M., El Hamri R., Taitai A., *J. Mater. Environ. Sci.* 5 (5) (2014) 1442-1453.
13. Zhou H., Bhaduri S. *J. Biomed. Mater. Res. B Appl. Biomater.* 100 (2012) 1142– 1150.
14. LeGeros R.Z., LeGeros J.P., Hench L.L., *New York World Scientific Press* (1998) 139-180
15. Zyman Z. Z. & Tkachenko M.V., *Processing and Application of Ceramics* 7 [4] (2013) 153–157.
16. Koutsopoulos S., *J. Biomed. Mater. Res.* 62 (2002) 600–612.
17. Meejoo S., Maneeprakorn W., Winotai P. *Thermochimica acta* 447 (2006) 115–120.
18. Gómez-Morales J., Iafisco M., Delgado-López J.M., Sarda S., Drouet C., *Progress in Crystal Growth and Characterization of Materials* 59 (2013) 1-46.
19. Antonakosa A., Liarokapisa E., Leventouri T. *Biomaterials*, 28 (2007) 3043–3054.
20. Sargin Y., Kizilyalli M., Tell C. & Güilef H. *Journal of the European Ceramic Society* 17 (1997) 963-970.
21. Bennani-Ziatni,M., Lebugle, A., Bonel, G. *Ann. Chim. Fr.* 16 (1991) 607-617.
22. Panda R. N., Hsierch M.F., Chung R.J. and Chin T. S., *J. Phys. Chem. Solids*, 62 (2003) 193.
23. Liao S., Xu, G., Wang W., Watari F., Cui F., Ramakrishna S., and Chan, C. K., *Acta Biomater.* 3(2007) 669-675.
24. Banfield, J. F., Welch, S. A., Zhang, H., Ebert, T. T., and Penn, R. L., *Science*, 289 (2000) 751-754.
25. Penn, R. L., and Banfield, J. F., *Science*, 281 (1998) 969-971.
26. Tao, J., Pan, H., Zeng, Y., Xu, X., and Tang, R., *J. Phys. Chem. B* 111 (2007) 13410-13418.
27. Melikhov I.V. *Inorg. Mater.* 36 (2000) 278–286.
28. Sergey V. Dorozhkin , *American Journal of Biomedical Engineering*, 2(3) (2012) 48-97

(2015) ; <http://www.jmaterenvirosci.com>